THE ASTRONOMICAL JOURNAL, 118:1252–1267, 1999 September

GALACTIC NEUTRAL HYDROGEN EMISSION PROFILE STRUCTURE

GERRIT L. VERSCHUUR
Department of Physics, University of Memphis, Memphis, TN 38152; gverschr@memphis.edu
AND
ANTHONY L. PERATT[1]
US Department of Energy, Washington, DC 20585 alp@lanl.gov
Received 1998 September 4; accepted 1999 May 25

ABSTRACT

Analysis of Galactic neutral hydrogen emission profiles that have been corrected for sidelobe radiation confirm the existence of three distinct component line width regimes identified by Verschuur & Magnani in 1994. In addition, a fourth becomes recognizable in the data in directions of low total column density. The line width regimes are around 50 km s^{-1} (component 1a), 31 km s^{-1} (component 1b), 13 km s^{-1} (component 2), and 5.2 km s^{-1} for the narrow lines arising from cool H I (component 3). In this paper, the new data are presented and compared with previously published results. The possible origin of the distinct line width regimes is briefly examined, and it is concluded that a new interpretation is needed, one that involves a plasma phenomenon known as the critical ionization velocity, which will be fully discussed in a subsequent paper.

Key words: ISM: atoms — ISM: general-ISM: H I — physical data and processes

1. INTRODUCTION

Interstellar neutral hydrogen (H I) emission-line profiles are generally complex features that appear to represent the superposition of several components individually Gaussian in shape. Verschuur & Schmelz (1989) used high-resolution H I profiles to identity several distinct line width regimes for these components. Narrow line widths from 3 to 6 km s^{-1} predominated in the sample of profiles they used for Gaussian analysis, with the histogram of the line widths suggesting a second peak around 13 km s^{-1}. A much broader line width regime in the 25–40 km s^{-1} range was also present in their data, and they cautiously suggested that a contribution to the emission profiles from stray radiation entering the sidelobes might have created the illusion of such a component.

Making use of data obtained on several telescopes, as well as extracting information from published H I profiles, Verschuur & Magnani (1994) subsequently extended the work of Verschuur & Schmelz (1989) and confirmed the existence of three distinct line width regimes in H I emission profiles: a broad component 1 with line widths ranging from 25 to 40 km s^{-1} and with some out to 50 km s^{-1}, component 2 with line widths around 12 km s^{-1}, and component 3 with line widths in the 2–6 km s^{-1} range due to cold H I. They also suggested that a contribution from sidelobes might be present in their data to generate the broad features making up component 1.

This paper considers the results of a Gaussian analysis of sidelobe-corrected data obtained as part of the Leiden-Dwingeloo all-sky H I survey, carried out by Hartmann & Burton (1995, hereafter the L-D Survey) which show that component 1 is physically real and has a line width of $\sim$31 km s^{-1}. Furthermore, sidelobe-corrected data obtained in directions of relative H I deficiency with the 140 foot (43 m) radio telescope by Lockman, Jahoda, & McCammon (1986) are Gaussian-analyzed, and these suggest the presence of an additional albeit very faint, component with a line width of $\sim$50 km s^{-1}. The L-D Survey data close to these same directions were also Gaussian-analyzed and confirm the statistical presence of both broad components. These two broad line width categories will be referred to as component 1a ($\sim$50 km s^{-1}) and 1b ($\sim$31 km s^{-1}), respectively. In addition, the sidelobe-corrected data sets show clearly that component 2 has a mean line width of $\sim$13 km s^{-1} and that component 3 has a mean line width of $\sim$5.2 km s^{-1}.

The study presented here concerns Gaussian components quite distinct from, and brighter than, those produced by a putative Galactic halo suggested by Kalberla et al. (1998). They describe an extremely weak underlying component with a line width of order 140 km s^{-1} and a peak brightness temperature of $\sim$0.05 K, which is well below the level of detection in the experiments discussed here.

In the present paper the H I data are discussed and the possible origin of the line width regimes considered. In a subsequent paper Peratt & Verschuur 1999), a new approach to the data first offered by Peratt & Verschuur (1998) suggests that the four line width categories be considered in the context of the critical ionization velocity (CIV) phenomenon in interstellar space, a phenomenon originally proposed by Alfvén (1942, 1954, 1960) and since studied in the laboratory and in interplanetary space (Brenning 1992a, 1992b).

It is stressed that one of us (G.L.V.) spent several years analyzing the shapes of H I emission profiles and pondering the meaning of the three basic line width regimes well before he learned of the existence of the CIV phenomenon. To that extent, the earlier data are free of bias in data analysis favoring component line widths that may lead to an association with any other physical phenomenon. The data obtained subsequently are largely from the L-D Survey and were studied in order to show whether the broad component 1 originally identified by Verschuur & Magnani (1994) was real. This latter analysis confirmed the existence of component 1, which raised the question of why H I profiles

[1] Permanent address: Los Alamos National Laboratory, Los Alamos, NM 87545.

could have a width so very much greater than any allowed by neutral gas, since the component 1 line width, if simply interpreted, implies that the neutral hydrogen has a physically impossible kinetic temperature of $\sim$52,500 K, since the gas would be fully ionized at this value.

2. THE INFORMATION CONTENT OF H I EMISSION PROFILES

Neutral hydrogen emission-line data can be presented in a variety of ways, each of which reveals some specific aspect of the physical processes that give rise to the emission. In the early days of H I studies (the 1950s and early 1960s) it was common to report emission profile shapes (spectra), which were then discussed in general terms, at best. When contour-mapping software and associated plotter hardware became available in the late 1960s and early 1970s, a new trend emerged. Maps of H I brightness as a function of velocity and position were published in large numbers (e.g., Westerhout 1966; Weaver & Williams 1973; Heiles & Habing 1974; Burton (1985). That, in turn, led to the production of area maps of H I brightness or column density as a function of two spatial coordinates being published in catalog form (e.g., Verschuur (1974a, 1974b; Colomb, Pöpell, & Heiles 1980; Burton & te Lintel Hekkert 1985). Such area maps of H I properties are readily compared with photographs or other area representations of astronomical data, such as the brightness of infrared 100 μm or 60 μm emission from interstellar cirrus dust (e.g., Boulanger & Perault 1988; Verschuur et al. 1992; Brown, Hartmann, & Burton 1995). These allow extensive qualitative comparison between, for example, H I column density and 100 μm brightness in order to learn about the underlying physics of the regions in which H I and cirrus dust coexist.

Today many databases containing H I survey profiles (e.g., Stark et al. 1992; Hartmann 1994; Hartmann & Burton 1995) are stored as data cubes. Slices across such cubes are extracted to plot brightness as a function of two spatial coordinates or one of space and one of velocity to suit a given project. Alternatively, a profile at any given point in the cube may be displayed.

It should be noted that area maps showing H I brightness at a given velocity or the H I column density are a simplistic representation of what is surely a complex underlying situation. They indicate the tips of the icebergs in a sense, because the structures that appear on such maps are seen in contrast against a background. This began to be revealed in part through the work of Verschuur & Schmelz (1989), who pointed out that typical H I profiles reflect the existence of two, possibly three, distinctly different component line widths regimes. The existence of such profile structure is not evident in area maps of H I emission at a given velocity or in total H I content.

Verschuur & Magnani (1994) showed that two broad line width components are widespread. They found that component 1 has line widths ranging from 25 to 40 km s^{-1} and that it occurs in every direction observed, which was also the case for component 2, with a line width around 12 km s^{-1}. Many directions were identified where these were the *only* two components in an emission profile. Component 3 includes narrow features from 2 to 6 km s^{-1} wide, and these are invariably superposed on component 2. The narrow components are *never* found as isolated profiles away from the velocity of the broader features. In general, component 3 appears associated with dust and sometimes molecular structures, but even this is not always so. Our interpretation of these observations is that in order to untangle the quantitative relationship between cool H I and dust, for example, the background contribution from broad components 1 and 2 should first be subtracted. It was while Verschuur (1994, 1995a, 1995b) was attempting to interpret H I area maps of several H I structures in this manner that he was forced to understand what gave rise to the three component line-width structure in the first place. That work inexorably led to the results reported here.

As Verschuur & Magnani (1994) noted, the possibility existed that component 1 might be produced by radiation entering the beam through sidelobes, and in this paper we will show that this is not the case. Although a small sidelobe contribution exists in all observed H I profiles, it turns out that after correcting the data for stray radiation, the *statistics* of component line widths are very little affected. While peak brightness temperatures of the fitted components will vary depending on how much of a sidelobe correction is applied relative to the peak brightness of the profiles, the statistical distribution of line widths and center velocities of the Gaussian components from ensembles of data defining the profiles are not significantly affected by such corrections.

We will investigate the nature of the basic Gaussian components that define a typical H I emission profile by analyzing data that were corrected for sidelobe contamination by Hartmann (1994), Hartmann & Burton (1995), and Lockman et al. (1986). It is found that the originally defined component 1 is real and that in directions of the sky where very little H I is seen a further distinction between a group of Gaussians with line widths around 50 km s^{-1} (component 1a) and those with line widths around 30 km s^{-1} (component 1b) may be made. In most cases component 1a is very difficult to identify, largely because its width is so great and its brightness temperature so low ($\sim$0.3 K), which means it may have been regarded as a "baseline" problem by many observers. Insufficient or imperfect baseline data will quickly prevent its presence from being recognized.

2.1. *A Basic Assumption*

We operate under a guiding assumption that H I emission profile structure carries information that has a bearing on the physics responsible for the emission. This point may seem too obvious to mention, but it is stated in the context of the modern trend to study area distribution of H I brightness and column density for comparison with dust or molecular structures without paying attention to the possible presence of an underlying background of emission. When this background is removed, as Verschuur (1994, 1995b) has found, the H I small-scale structure observed with a single-dish radio telescope looks a great deal more like the cirrus distribution than it does on maps of total H I content, or even peak brightness at any given velocity. However, the process of identifying and removing this background component in H I is difficult and time-consuming; it has to be done profile by profile. At the same time, the presence of a "background" of cirrus emission must also be considered. If this correction to the H I data is not done, the quantitative relationship between gas and dust may be off by as much as an order of magnitude, since the cool component 3 may represent less than 10% of the total H I column density in the emission profile (see below).

It is our goal to understand the information carried in H I emission profile structure. To do so requires extensive Gaussian analysis of H I emission spectra to characterize their basic nature, and this assumes that Gaussians are a valid way of performing this characterization. To first order, this is still a basic tenet in the study of interstellar matter: the mass motion of the atoms of H I gas at a given kinetic temperature is random with a velocity spread determined by that temperature. This produces an emission profile shape that reveals a normal or Gaussian distribution. Even if there should be some hidden reason for this basic assumption to be incorrect, our experience of the relevant data analysis is such that the Gaussian analysis nevertheless allows us to characterize general properties of gas from region to region in the sky, and it allows us to draw conclusions based upon similarities and differences in the profile shapes that can be quantified in terms of the superposition of a number of Gaussians.

2.2. *On the Nature of Gaussian Fitting*

H I emission profiles contain a wealth of physical information encapsulated within the individual Gaussian parameters, and the challenge is to read the message in terms of those parameters. Such information can only be extracted by paying attention to the data in a hands-on manner. This is not something that can be left to an idealized computer program, which does its job without paying attention to patterns that may be common over a particular area of sky or structural properties that differ from one area of sky to another.

To remove the human mind from the analysis is to cut ourselves off from seeing what may be the crucial clues that might allow the nature of interstellar gas structure and dynamics to be untangled. To state this in another way, in all Gaussian analysis a judgment must be made about where to start and where to stop by way of choosing parameters for the minimum number of Gaussians required to represent a given profile. This can be approached in either a mindful manner (using one's senses) or a mindless manner (attempting a fully automated approach). The latter has a far greater likelihood of producing a mindless result. The computer can and should only be used for honing the final fit.

There are critics who claim that the mindful manner will always be biased. In our defense, we note that the conclusions presented here are based on experience garnered by one of us (G.L.V.) after fitting over 7000 Gaussian components to H I profiles, most of which took many iterations before a final set of parameters was handed over to software for a final derivation. The probability that a systematic error of an egregious sort could survive this process is extremely unlikely. We assume that nature is reasonable and that a mindful look at the data will give a reasonable indication about what nature is doing.

Nevertheless, a key question that must be confronted in any study involving Gaussian analysis of complex H I emission profiles is whether the Gaussian fit for any given profile is unique. Note that this study is limited to the analysis of relatively simple profiles for which an initial set of parameters could readily be chosen. Apart from the thin filament area of sky (§ 5.4) where the profiles were sometimes quite complex and extended by as much as 60 km s^{-1} in velocity, a typical profile required three to four components for its full characterization. It is well known to those who have attempted Gaussian analysis of this sort that one must begin by suggesting a set of likely Gaussian parameters before a computer can complete a fit in a statistical manner. Also, the smaller the number of components that provide a good fit, the more unique the solution is likely to be.

The first step in choosing a set of Gaussians for a given profile requires that we use all the information available to the eye as regards profile structure, taking into account the nature of the wings in the profile and the presence of changes in slope that deviate from Gaussian at the sides of the profiles. The point is that nature provides us with this information, and we should make use of it.

In the analysis discussed here, the first Gaussian component chosen to characterize any profile (the original component 1) accounts for the emission in the profile wings, following the steps outlined by Verschuur & Schmelz (1989). To do otherwise, for example, by starting with the bright peaks, is to invite being trapped into an endless regression of Gaussians required to fit the details in the profile. After the first broad component was subtracted, a second Gaussian component was fitted to account for the next-broadest component and subtracted. Any emission left over was invariably due to one, and sometimes two, much narrower components. If two are present, they are usually clearly separated in velocity compared with their narrow line width, which then makes their identification unambiguous. These statements are true for all the relatively simple profiles studied here.

The *minimum* number of Gaussians required to produce a residual equivalent to the noise at velocities outside the profile were always fitted to the profiles. If this restraint were not imposed, one could, in the limit, fit Gaussians to every noise spike, which would be absurd. It turns out that for most of the H I profiles studied here, all of which were observed at Galactic latitudes above 15°, from two to six Gaussians account for all the observed profiles, with the vast majority requiring three or four.

Since the Gaussian fitting for the best data sets was always completed by computer, the role of observer bias in the final judgment as to a best fit was minimized. Also, in our analysis we only made use of the line width data for the Gaussian components and did not attempt to extract information from the distributions of peak amplitudes, center velocities, or column densities other than what is offered in § 5.6. While Gaussian fits for emission profiles observed with different telescopes in the same direction of the sky may vary, the largest differences tend to be in peak temperatures, while central velocities are usually similar if not identical. It was found that the Gaussian line width statistics are affected least of all (see § 3.4).

Finally, we avoided reanalyzing those profiles for which the Gaussian fits did not accord with the subsequently identified component categories. We simply performed the best fit possible on each profile and then looked at the raw statistics of the results. This aspect of the analysis is particularly relevant in the context of Gaussian fitting done to data sets obtained before 1995, which at the time were not intended for use in anything like the present study.

3. OVERVIEW OF THE DATA AND THE GAUSSIAN ANALYSIS

3.1. *Summary of Observations*

Our goal was to determine whether the three line width

components defined by Verschuur & Magnani (1994) are present in the sidelobe-corrected L-D Survey. For this, profiles from the L-D database were extracted for regions previously mapped by Verschuur (1994, 1995b) using the Arecibo radio telescope, so that line width statistics could be compared. Earlier results of the Gaussian analysis of the Arecibo profiles have been reported by Verschuur & Magnani (1994). By at first limiting our study of the L-D Survey data to the same regions, we were able to examine the consequence of resolution, as well as sidelobe correction, on the Gaussian analysis.

We did not extend the study to the broad-beamwidth, low-sidelobe H I profiles published in the Bell Labs survey (Stark et al. 1992). When too large an area of sky is included in a beam, the profiles begin to blend to such an extent that component structure is rapidly lost. Based on our study of small areas of sky with high resolution it is clear that the H I structure is so complex that in the 2°.5 beam of the Bell Labs survey a great deal of information on crucial line structure, and hence on the relative presence of the four Gaussian component regimes discussed here, may be lost.

3.2. *Gaussian Fitting to the Profiles*

Table 1 summarizes the various data samples used in the discussions to follow. Gaussian analysis of nearly 1700 H I emission profiles produced nearly 8000 component line widths. In the case of the analysis of the L-D Survey data, the profiles were examined, and the parameters describing the most likely Gaussian components were adjusted until a fit that reduced the residual to the level of noise outside the profile range was achieved. The final fit was calculated by computer. Extensive tests were done by comparing the results of Gaussian fitting done by iterating manually until the residual reached the level of noise outside the profile bounds with those rounded off by computer. It was found that the "hands-on" approach usually yielded results that were so close to those found by computer fitting as to be discernible only by the computer. Line widths seldom differed by a few percent. Nevertheless, for all the crucial data discussed here, the final fit by computer was used to quantify the parameters used in this study. In tests performed on a number of profiles using different starting points, the line width results were again found to agree to better than a few percent. It is stressed that it is the line width *statistics* emerging from these data that are at issue, not the absolute value of the parameters defining specific Gaussian components.

Figure 1 is an example of an archetypal profile from the L-D Survey at $l = 119°.0$, $b = -78°.0$ in which one each of components 1b, 2, and 3 is manifested. It shows the Gaussian fit rounded off by computer and the difference that remained. Apart from a slight bump around -45 km s^{-1}, which we did not treat, this profile shows the three components present to about the same amplitude, a rare situation.

3.3. *Random Directions from the L-D Survey*

Since much of the study described here initially concentrated on directions of the sky previously studied for specific, albeit unrelated, reasons, it was felt that the apparent existence of the three component regimes in the L-D Survey data should be considered more generally by performing a Gaussian analysis of profiles in directions chosen at random. A random number generator was therefore used to pick 49 directions distributed over the sky visible in the Northern Hemisphere and with $|b| > 15°$. The coordinates for these profiles are listed in Table 2. The relevant emission profiles were then taken from the L-D Survey, and the profiles in all but three directions were Gaussian-analyzed. The exceptions were too bright and complex for a meaningful analysis to be performed.

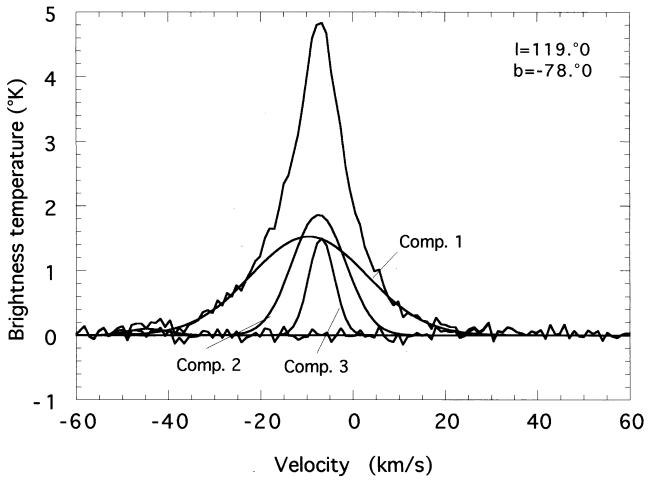

FIG. 1.—Gaussian fit to the L-D Survey profile at $l = 119°$, $b = -78°$. The three components are each represented just once, and at about the same amplitude. The residual left after subtracting the three components from the data is also indicated. No attempt was made to account for the feature at -45 km s^{-1}.

3.4. *On the Quality of Gaussian Fitting*

Figures 2*a–d* give examples of Gaussian fits to the some of the L-D Survey data for the random position profiles. A very good fit is obtained using one each in the component 1b, 2, and 3 line width categories without any suggestion of added complexity. They show how the basic component categories are readily and unambiguously identified in simple profiles. Further examples are given in Figures 3*a–b*, two profiles in directions chosen because of their low H I column density (see § 5.3). These fits were done to relatively noisy data and are good examples of the quality of the fits to weaker emission lines.

Table 3 gives the Gaussian parameters fit to the profiles shown in Figures 2 and 3 and Figure 5 below. Column densities are also given, and in the last column the percentage of H I in a cool component 3 compared with the total column density for that profile is shown. It is the cool component that is found to be associated with the bright interstellar cirrus structures, and these examples illustrate that to make meaningful quantitative comparisons between cold gas and dust the "background" emission due to components 1 and 2 in H I, as well as a background cirrus contribution, must be considered before such a comparison is carried to a conclusion.

3.5. *Are the Gaussian Fits Unique?*

A question remains as to whether any given Gaussian fit to an H I emission profile is unique. Based on experience and concentrating only on directions in the sky where there is relatively little H I emission away from the Galactic plane, the component fitting choice is dictated by the structure

TABLE 1

AREAS OF SKY FOR WHICH GAUSSIAN ANALYSIS WAS PERFORMED.

A. LEIDEN-DWINGELOO SURVEY DATA

SAMPLE	APPROXIMATE				NUMBER OF L-D PROFILES	NUMBER OF GAUSSIANS	NUMBER OF ARECIBO PROFILES
	R.A.	Decl.	Long.	Lat.			
H0928+10	9 28	+10	232	+36	12	54	300
H0827+02	8 27	+2	215	+25	25	126	75
H1025+05	10 25	+5	238	+50	16	64	100
MBM 12	2 54	+20	158	−34	9	54	...
UMa	9 30	+72	141	+38	9	37	...
Random directions					50	240	...
Low H I column density directions					12	51	...
Thin filament	14 34	+35	58	+67	247	1695	...
Subtotal					380	2321	

B. Other Data Referred to in Text

Source	Number of Profiles	Number of Gaussians
Sidelobe-corrected profiles (Lockman et al. 1986)	12	63
Sample from Verschuur & Magnani 1994	1012	3692
Sample from Verschuur & Schmelz 1989	172	727
Sample from Verschuur 1995c observations obtained in 1992	75	310
Thin-filament data obtained in 1997	36	179
Total of all data	1687	7692

NOTE—Units of right ascension are hours and minutes (B1950.0), and units of declination, latitude and longitude are degrees.

TABLE 2

RANDOM DIRECTIONS CHOSEN FROM THE LEIDEN-DWINGELOO DATA FILES

Longitude (deg)	Latitude (deg)	Longitude (deg)	Latitude (deg)	Longitude (deg)	Latitude (deg)
183.0.....	76.5	242.0.....	76.5	65.5	76.5
63.5	74.0	125.5.....	70.0	6.5	71.5
266.5.....	64.5	359.0.....	60.5	245.0.....	60.5
127.0.....	57.5	223.0.....	56.0	283.0.....	54.5
230.0.....	54.0	238.5.....	52.0	83.0	52.0
232.5.....	51.5	24.0	51.5	62.0	51.0
233.0.....	50.0	129.0.....	47.0	265.5.....	46.5
43.0	41.5	51.0	41.0	22.5	41.0
133.5.....	36.5	122.5.....	33.0	24.0	32.5
121.5.....	29.5	211.0.....	28.0	40.0	23.0
99.5	22.5	120.0.....	21.0	164.0.....	17.0[a]
160.0.....	16.0	142.0.....	−15.5	155.5.....	−16.5
86.0	−18.5	197.0.....	−19.5	47.0	−20.5
204.5.....	−25.0	175.5.....	−33.5[a]	130.0.....	−35.0
85.5	−36.5	125.5.....	−38.0	168.0.....	−39.0[a]
88.0	−57.0	115.5.....	−64.0	107.0.....	−65.0
119.0.....	−78.0				

[a] Profile too complex to allow Gaussian fitting.

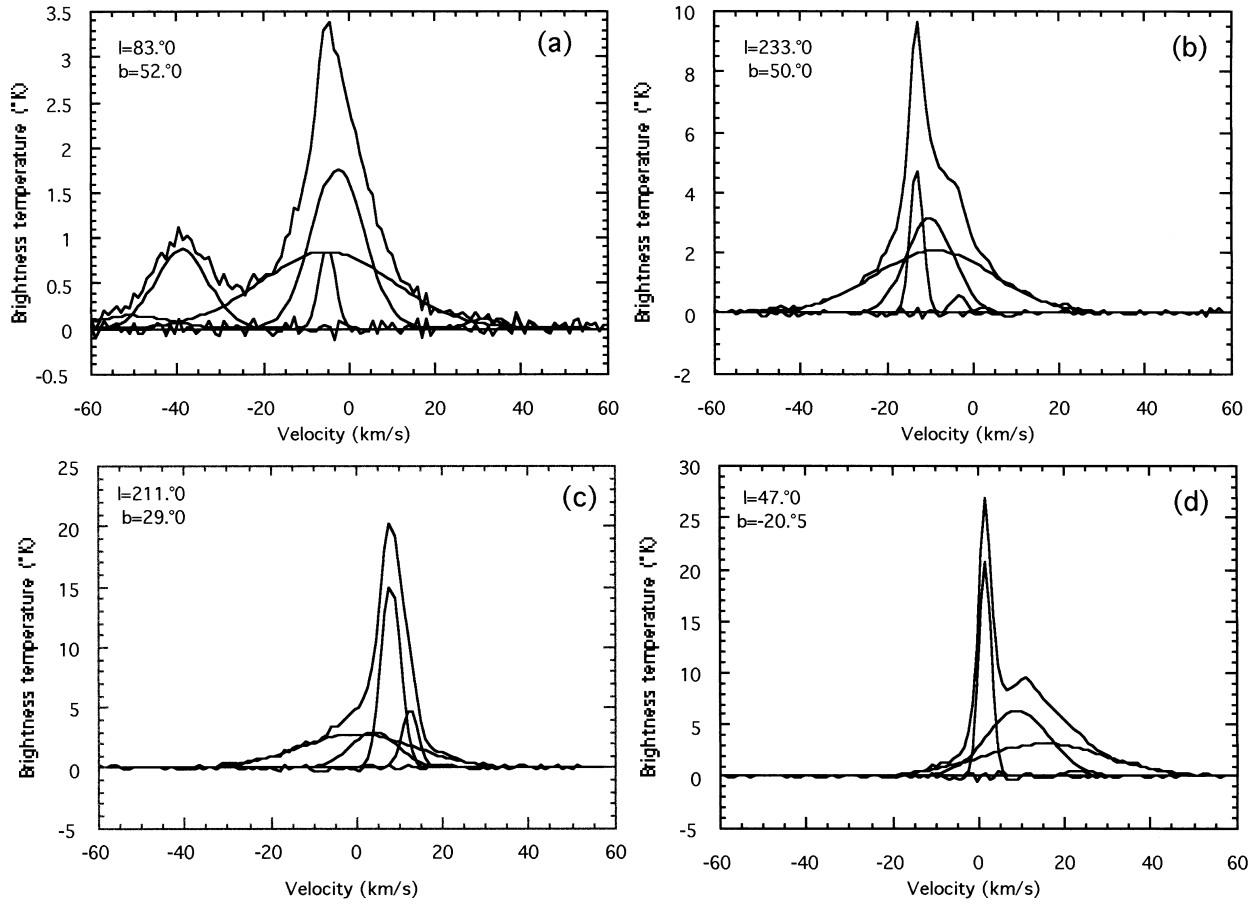

FIG. 2.—Gaussians fitted to the L-D Survey profile for a number of directions. Component parameters are given in Table 3. (*a*) For $l = 83\overset{\circ}{.}5$, $b = 52\overset{\circ}{.}0$, showing the presence of components 1b, 2, and 3. The peak around -40 km s^{-1} has a line width corresponding to component 2. As was generally true in our study, possible weak components at center velocities less than -50 were not included in the analysis. (*b*) For $l = 233\overset{\circ}{.}0$, $b = 50\overset{\circ}{.}0$, showing the presence of components 1b and 2 and three examples of narrow component 3; one of them, at 2.5 km s^{-1}, is extremely weak. (*c*) For $l = 211\overset{\circ}{.}0$, $b = 28\overset{\circ}{.}0$, showing the presence of components 1b, 2, and two examples of narrow component 3. (*d*) For $l = 47\overset{\circ}{.}0$, $b = -20\overset{\circ}{.}5$, showing the presence of components 1b, 2, and 3. The slight ripple in the residual may indicate the presence of an additional feature of the component 3 variety, but to first order the fit is satisfactory and shows how component 1b is required to account for the wings of the profile.

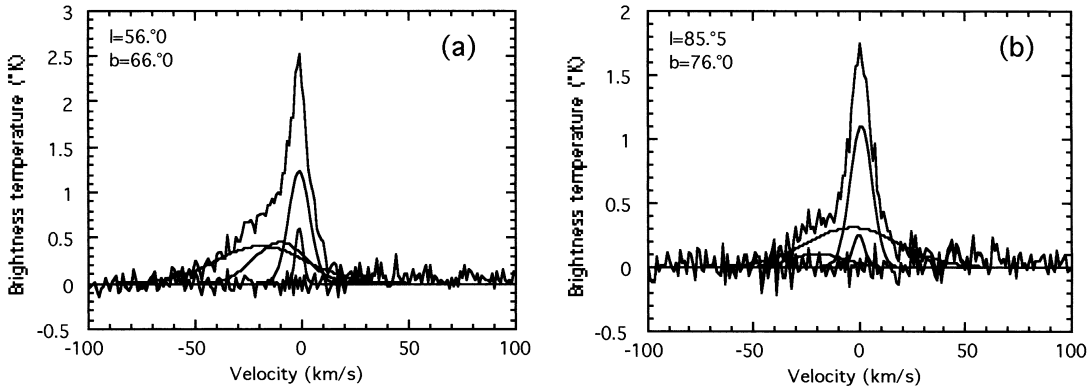

FIG. 3.—Gaussians fitted to L-D Survey profiles with low column densities. (*a*) For $l = 56\overset{\circ}{.}0$, $b = 66\overset{\circ}{.}0$. No attempt was made to subtract a baseline, which probably accounts for the slightly positive levels of the noise at velocities greater than 24 km s^{-1}, which was the limit of the fitting to this profile. Here all four basic component categories are present (see Table 3). (*b*) For $l = 85\overset{\circ}{.}5$, $b = 76\overset{\circ}{.}0$. No attempt was made to subtract a baseline, which probably accounts for the slightly positive levels of the noise at velocities greater than 40 km s^{-1}, which was the limit of the fitting to this profile. Here all four basic component categories are present (see Table 2).

in the profile to such an extent that little ambiguity is possible. This is evident in Figures 2 and 3, and the other L-D profiles analyzed in this study gave very similar results. Four Gaussian components were usually enough to fully characterize the vast majority of the profiles considered here; one each of the wide components (32 and 13 km s^{-1}) and one or two narrow components. Since our study was restricted to analysis of simple profiles at intermediate and high Galactic latitudes, we are confident that systematic errors due to limitations in the Gaussian-fitting protocol are minimized.

4. THE NATURE OF THE SIDELOBE SIGNALS

In order to better understand the extent to which sidelobe signals might have affected the data obtained with the Arecibo 309 m radio telescope and the 140 foot radio telescope of the National Radio Astronomy Observatory (Verschuur & Magnani 1994) in the past, we performed tests on L-D Survey profiles before and after sidelobe corrections were applied. The results may be summarized as follows: to first order, the near- and far-sidelobe corrections made by Hartmann (1994) play little if any role in affecting the *statistics* of the line widths derived from a Gaussian analysis. The sidelobe corrections make very little difference to a profile *shape* at the levels of brightness temperature with which we are concerned. The sidelobe correction profiles that were examined, which combine contributions from near and far sidelobes, produce a corrected profile in brightness temperature that looks very much like the observed profile when plotted in antenna temperature in the sample we examined carefully. In other words, both components 1 and 2 are present in the raw data for the L-D Survey and the corrected data at the same amplitude (coincidentally), except that the former data are measured in antenna temperature and the latter in brightness temperature.

From this study we conclude that about 25% of the *amplitude* of component 1 appears to come from radiation in the near and far sidelobes, but that does little to affect the line width statistics. As the subsequent analysis showed, component 2 appears to be physically real and is in no way related to the presence or absence of sidelobe radiation.

4.1. *Intertelescope Comparisons*

A detailed comparison using data obtained by two very different telescopes was made of the results of Gaussian analysis for the first three regions listed in Table 1. These features are brightness concentrations along a filament described by Verschuur (1991a, 1991b) and were part of a high-resolution mapping project carried out at the Arecibo Observatory, which led to our confrontation of the nature of H I emission profile structure in the first place. The regions are called H0827+10 (G215+25), H0928+02 (G231.5+35.5), and H1025+05 (G238+50), with the names referring either to their approximate right ascension and declination or Galactic longitude and latitude.

The L-D Survey data for each area were also Gaussian-fitted, and Tables 4, 5, and 6 give the results of numerical comparisons between these results and those obtained from Gaussian analysis of the raw Arecibo observations. In these tables, the average parameters and a 1 σ error for each group of Gaussians identified with a certain component are shown.

Table 4 gives the results for the Gaussian component fits for the H0827+10 region. The results indicate that Gaussian analysis of data obtained with a 4′ beam (subject to sidelobe signals) produce profiles whose general characteristics are similar to those found from Gaussian analysis of data obtained with a 36′ beam (sidelobe-corrected) for the same area of sky. The results of Gaussian fitting to the H0928+02 region and comparison with Arecibo results are shown in Table 5. The third region for which the comparison was carried out is H1025+05 (Table 6), originally chosen for mapping because it is a direction in which H I contour maps show virtually no structure (Verschuur 1974a). Also, the *IRAS* 100 μm data show virtually no structure here either. For this reason, the Arecibo profiles are very simple, usually consisting of one or two weak, narrow components on top of dominant components 1b and 2 and often showing no narrow components at all.

The data in these three tables indicate that the different line width regimes identified by (Verschuur & Magnani (1994), components 1b, 2 and 3, can clearly be recognized in the emission profiles from the L-D Survey data. This implies that the line width statistics obtained from uncor-

TABLE 3

GAUSSIAN PARAMETERS FOR PROFILES SHOWN

Position and Component Category	Brightness Temperature (K)	Center Velocity (km s^{-1})	Line Width (FWHM) (km s^{-1})	Column Density (10^{18} cm^{-2})	Fraction of H I in Comp. 3
Sample of Profiles in Random Directions					
$l = 119\overset{\circ}{.}0$, $b = -78\overset{\circ}{.}0$ (see Fig. 1):					
Component 1b.....	1.5	−9.5	29.6	82.8	
Component 2	1.9	−7.4	13.7	46.6	
Component 3	1.5	−6.8	6.5	18.0	0.12
Component 2	0.1	−44.6	10.2	1.9	
Total				149.2	
$l = 83\overset{\circ}{.}0$, $b = 52\overset{\circ}{.}0$ (see Fig. 2*a*):					
Component 1b.....	0.8	−5.2	36.5	56.6	
Component 2	1.8	−2.6	14.5	46.9	
Component 3	0.9	−5.1	4.3	6.9	0.05
Component 2	0.9	−39.0	14.5	23.2	
Blend?	0.1	−50.6	20.5	5.4	
Component 3	0.1	31.4	9.4	1.7	0.01
Total				140.8	
$l = 233\overset{\circ}{.}0$, $b = 50\overset{\circ}{.}0$ (see Fig. 2*b*):					
Component 1b.....	2.1	−9.0	32.8	124.8	
Component 2	3.2	−10.1	12.8	74.0	
Component 3	4.8	−13.2	3.7	32.5	0.14
Component 3	0.6	−3.4	3.6	4.1	0.02
Component 3	0.2	2.5	5.2	1.8	0.01
Component 3	0.1	−46.0	9.1	1.7	0.01
Total				238.8	
$l = 211\overset{\circ}{.}0$, $b = 28\overset{\circ}{.}0$ (see Fig. 2*c*):					
Component 1b.....	2.8	0.4	32.5	169.5	
Component 2	3.6	5.5	13.4	87.3	
Component 3	14.4	8.0	5.1	133.3	0.32
Component 3	4.4	12.3	3.9	31.7	0.08
Total				421.7	
$l = 47\overset{\circ}{.}0$, $b = -20\overset{\circ}{.}0$ (see Fig. 2*d*):					
Component 1b.....	3.1	15.3	34.6	194.0	
Component 2	6.4	9.0	17.4	204.5	
Component 3	20.7	1.5	3.5	133.9	0.25
Component 3	0.6	22.2	6.1	7.0	0.01
Total				539.4	
Sample of Profiles in Direction of Low H I Column Density					
$l = 56\overset{\circ}{.}0$, $b = 66\overset{\circ}{.}0$ (see Fig. 3*a*):					
Component 1a	0.4	−19.4	50.6	37.8	
Component 1b.....	0.5	−10.4	28.5	23.6	
Component 2	1.2	−1.3	12.1	27.3	
Component 3	0.6	−1.3	4.3	4.8	0.05
Total				93.5	
$l = 85\overset{\circ}{.}5$, $b = 76\overset{\circ}{.}0$ (see Fig. 3*b*):					
Component 1a	0.3	−3.3	50.7	28.6	
Component 1b.....	0.1	−19.6	28.0	5.4	
Component 2	1.1	0.6	12.4	25.0	
Component 3	0.3	−0.6	6.4	3.0	0.05
Total				62.1	
$l = 183\overset{\circ}{.}0$, $b = 62\overset{\circ}{.}0$ (see Fig. 5*b*):					
Component 1b.....	0.6	−3.8	34.0	37.8	
Component 2	0.8	−14.4	14.0	21.7	
Component 1b.....	0.1	−50.8	30.8	7.7	
Component 2	1.0	−54.2	14.9	26.5	
Component 2	0.2	−64.9	11.5	4.6	
Component 2	0.2	−39.5	10.2	4.4	
Component 3	0.3	−7.8	5.0	2.4	0.02
Total				105.1	

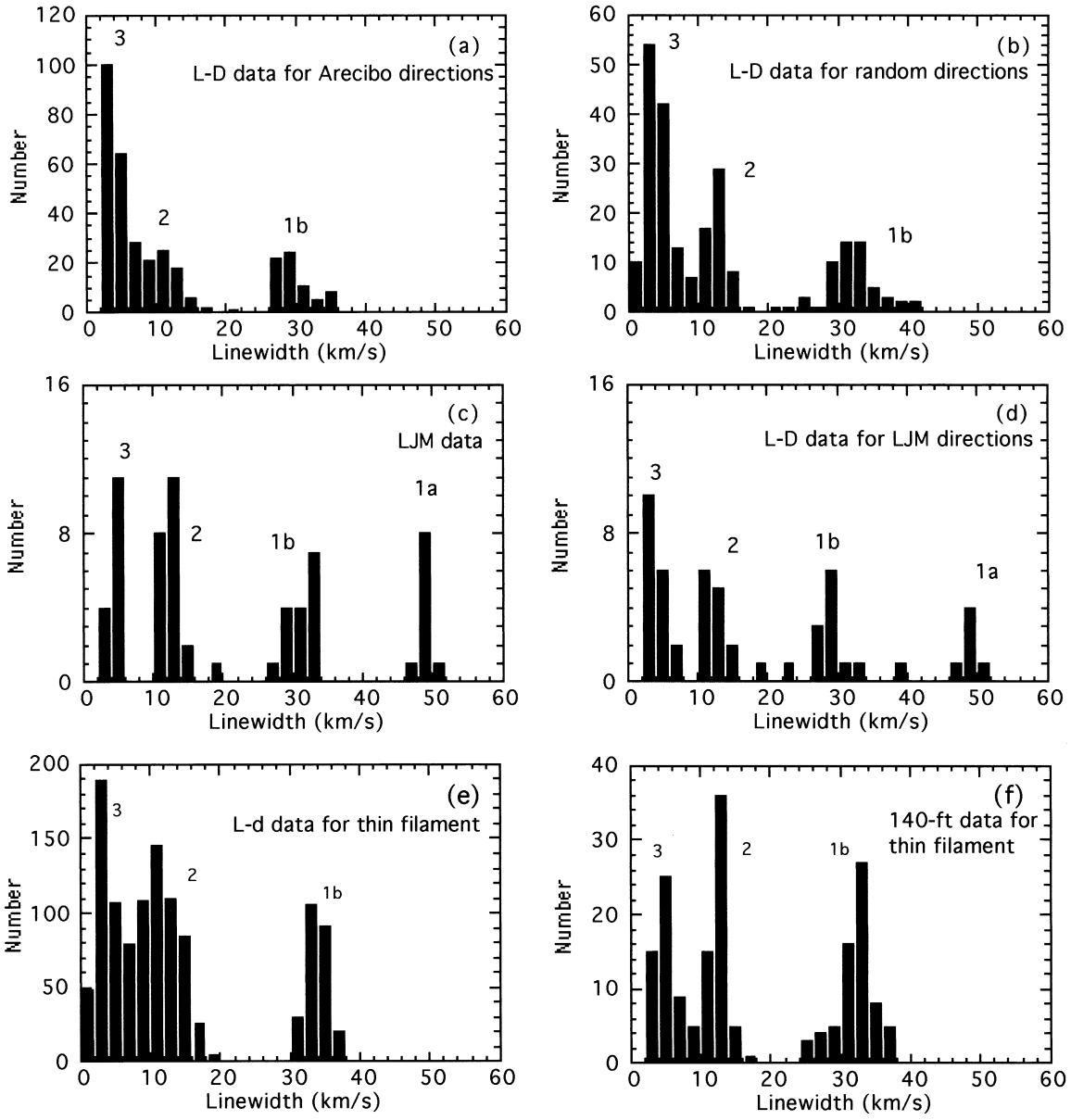

FIG. 4.—Histograms of component line widths for H I emission profiles discussed in this paper plotted in intervals of 2 km s^{-1}. (*a*) From the L-D Survey data for regions previously studied with the Arecibo radio telescope (see § 5). (*b*) From the L-D Survey data for a random sample of 46 directions (see § 5.2). (*c*) Gaussian fits to the 12 profiles obtained by Lockman et al. (1986) in directions of very low H I column density (see § 5.3). (*d*) From the L-D Survey profiles obtained at or close to the directions observed by Lockman et al. (1986) (see § 5.3). (*e*) From the L-D Survey data for the region of the thin filament (see § 5.4). (*f*) From data obtained with the 140 foot radio telescope data for the region of the thin filament (see § 5.4). The three line width component regimes around 30 km s^{-1} (component 1b), 12 km s^{-1} (component 2), and 3–6 km s^{-1} (component 3) are clearly revealed in all the data sets, confirming the identification by Verschuur & Magnani (1994) using data affected by sidelobe signals. In (*c*) and (*d*), an additional line width regime around 50 km s^{-1} becomes apparent.

rected profiles in the past (Verschuur & Schmelz 1989; Verschuur & Magnani 1994) are a fair representation of the fundamental nature of H I emission profile velocity structure. In particular, what we now label component 1b, while originally suspected of suffering from a sidelobe contribution, is clearly present in the L-D Survey data that were corrected for sidelobe radiation.

5. RESULTS OF THE GAUSSIAN ANALYSIS

5.1. *The Key Sidelobe-corrected Data Sets*

Figure 4*a* shows the line width histogram for all the Gaussian components fitted to the L-D Survey profiles for the three regions referred to in Tables 4–6, as well as for those Gaussians fitted to the sample of profiles examined for the Ursa Major region and MBM 12 (Table 1). The three component regimes are indicated. The data are summarized in Table 7. Note that component 2 for the Ursa Major region seems to be significantly lower than for the other regions, a phenomenon that may have a bearing on the interpretation to be presented in the subsequent paper (Peratt & Verschuur 1999).

5.2. *Random Directions Sampled in the L-D Survey*

Figure 4*b* plots the histogram of line widths of the Gaussians fitted to the profiles in the 47 random directions discussed above. The plot includes only those components with center velocity greater than -50 km s^{-1} and bright-

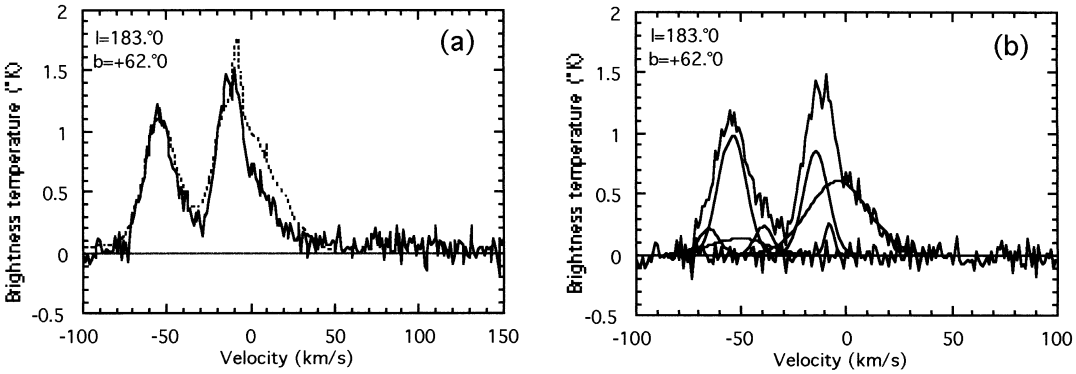

FIG. 5.—H I emission profiles observed toward $l = 183.^{\circ}0$, $b = 62.^{\circ}0$. (*a*) Profile from the L-D Survey data (*solid line*) and the one used by Spitzer & Fitzpatrick (1993) taken from Danly et al. (1986), (*dashed line*). No baselines have been removed from these profiles. Note the considerable difference between the two profiles at velocities greater than -15 km s^{-1}. (*b*) Gaussians fitted to the L-D Survey profile toward $l = 183.^{\circ}0$, $b = 62.^{\circ}0$ after removal of a linear baseline.

ness temperature above 0.15 K. The three line width regimes are again strikingly evident; component 1b is around 32–34 km s^{-1} wide, component 2 around 13 km s^{-1}, and component 3 peaks around 3–6 km s^{-1} (see Table 7).

5.3. *Profiles in Directions of Low* H I *Column Density*

A set of sidelobe-corrected H I profiles in 12 directions listed in Table 8 was published by Lockman et al., (1986). These were digitized and Gaussian-analyzed, and Figure 4*c*

TABLE 4

GAUSSIAN PARAMETERS OBTAINED FOR H0827+10 REGION FROM DATA OBTAINED WITH TWO TELESCOPES

Parameter	Arecibo (75 profiles)	L-D Data (25 Profiles)
Component 1 (b):		
Peak temperature (K)	2.3 ± 0.5	1.6 ± 0.5
Center velocity (km s^{-1})	4.7 ± 1.7	10.4 ± 1.3
Line width (km s^{-1})	29.5 ± 4.0	30.9 ± 3.7
Component 2:		
Peak temperature (K)	3.2 ± 0.4	5.0 ± 1.3
Center velocity (km s^{-1})	3.2 ± 0.3	2.1 ± 1.2
Line width (km s^{-1})	11.0 ± 0.3	11.3 ± 1.1
Component 3 (narrow components):		
Purple:		
Peak temperature (K)	1.5 ± 0.7	2.2 ± 1.6
Center velocity (km s^{-1})	0.0 ± 1.1	− 0.2 ± 0.8
Line width (km s^{-1})	3.8 ± 0.8	4.4 ± 0.8
Orange:		
Peak temperature (K)	3.5 ± 2.6	4.9 ± 4.7
Center velocity (km s^{-1})	3.3 ± 1.3	5.1 ± 1.6
Line width (km s^{-1})	3.6 ± 0.5	4.7 ± 0.5
Red:		
Peak temperature (K)	9.3 ± 6.7	4.9 ± 6.0
Center velocity (km s^{-1})	7.2 ± 0.6	7.5 ± 0.6
Line width (km s^{-1})	3.5 ± 0.6	4.5 ± 1.5
Green:		
Peak temperature (K)	1.1 ± 0.3	2.3 ± 2.5
Center velocity (km s^{-1})	14.7 ± 1.0	14.0 ± 0.9
Line width (km s^{-1})	6.0 ± 1.0	6.9 ± 1.7
Blue:		
Peak temperature (K)	1.2 ± 0.6	1.1 ± 0.6
Center velocity (km s^{-1})	22.7 ± 1.3	20.3 ± 1.8
Line width (km s^{-1})	5.6 ± 2.3	7.1 ± 1.0

TABLE 5

GAUSSIAN PARAMETERS OBTAINED FOR H0928+02 REGION FROM DATA OBTAINED WITH TWO TELESCOPES

Parameter	Arecibo (300 profiles)	L-D Data (12 Profiles)
Component 1 (b):		
Peak temperature (K)	2.4 ± 0.8	1.2 ± 0.4
Center velocity (km s^{-1})	−2.1 ± 1.0	− 2.9 ± 1.4
Line width (km s^{-1})	29.0 ± 2.9	30.7 ± 0.8
Component 2:		
Peak temperature (K)	5.1 ± 0.8	6.5 ± 0.4
Center velocity (km s^{-1})	−1.0 ± 0.6	− 1.5 ± 0.6
Line width (km s^{-1})	12.2 ± 0.7	13.2 ± 0.6
Component 3 (narrow components):		
M:		
Peak temperature (K)	8.6 ± 2.9	7.4 ± 6.0
Center velocity (km s^{-1})	0.1 ± 1.0	− 0.8 ± 0.7
Line width (km s^{-1})	4.0 ± 0.8	3.9 ± 1.0
A:		
Peak temperature (K)	2.8 ± 2.9	10.6 ± 4.5
Center velocity (km s^{-1})	3.5 ± 1.5	1.1 ± 0.5
Line width (km s^{-1})	5.0 ± 1.4	5.1 ± 0.9
B:		
Peak temperature (K)	0.4 ± 0.9	3.8 ± 2.7
Center velocity (km s^{-1})	7.2 ± 1.6	6.0 ± 1.1
Line width (km s^{-1})	3.9 ± 1.1	4.7 ± 0.9
C:		
Peak temperature (K)	0.6 ± 1.8	0.7 ± 0.3
Center velocity (km s^{-1})	−2.0 ± 0.9	− 8.8 ± 0.4
Line width (km s^{-1})	3.3 ± 0.5	6.5 ± 0.1

shows the line width histogram for this data set. In addition to those components with line widths around 32, 13, and 6 km s^{-1}, it appears that a fourth component may be present with a line width around 50 km s^{-1} (Table 7). In order to test whether this very broad component might be an artifact of the sidelobe correction applied by Lockman, et al. (1986), profiles obtained as close as possible to these directions were extracted from the L-D Survey and also Gaussian-analyzed. Since the L-D Survey produced profiles in a 0°.5 grid, this sample of directions is of course not identical. Figure 4*d* shows the histogram of Gaussian line widths so derived, which reveals the same four line width regimes seen in Figure 4*c*, with component 1a around 50 km s^{-1} and component 1b around 30 km s^{-1} wide.

TABLE 6

GAUSSIAN PARAMETERS OBTAINED FOR H1025+05 REGION FROM DATA OBTAINED WITH TWO TELESCOPES

Parameter	Arecibo (~100 Profiles)	L-D Data (16 Profiles)
Component 1 (b):		
Peak temperature (K)	1.7 ± 0.3	1.4 ± 0.3
Center velocity (km s^{-1})	−6.4 ± 1.3	− 6.1 ± 1.6
Line width (km s^{-1})	32.8 ± 3.7	31.2 ± 2.1
Component 2:		
Peak temperature (K)	3.0 ± 0.6	3.3 ± 0.6
Center velocity (km s^{-1})	−6.7 ± 0.5	− 7.6 ± 1.8
Line width (km s^{-1})	13.2 ± 0.5	14.9 ± 1.5
Component 3 (narrow components):		
Peak temperature (K)	0.9 ± 0.5	1.6 ± 0.7
Center velocity (km s^{-1})	−3.9 ± 0.5	− 4.8 ± 0.9
Line width (km s^{-1})	5.0 ± 1.3	6.0 ± 1.0
Peak temperature (K)	1.1 ± 0.4	1.6 ± 1.2
Center velocity (km s^{-1})	−14.1 ± 1.2	− 13.7 ± 0.6
Line width (km s^{-1})	5.0 ± 1.4	5.6 ± 1.1

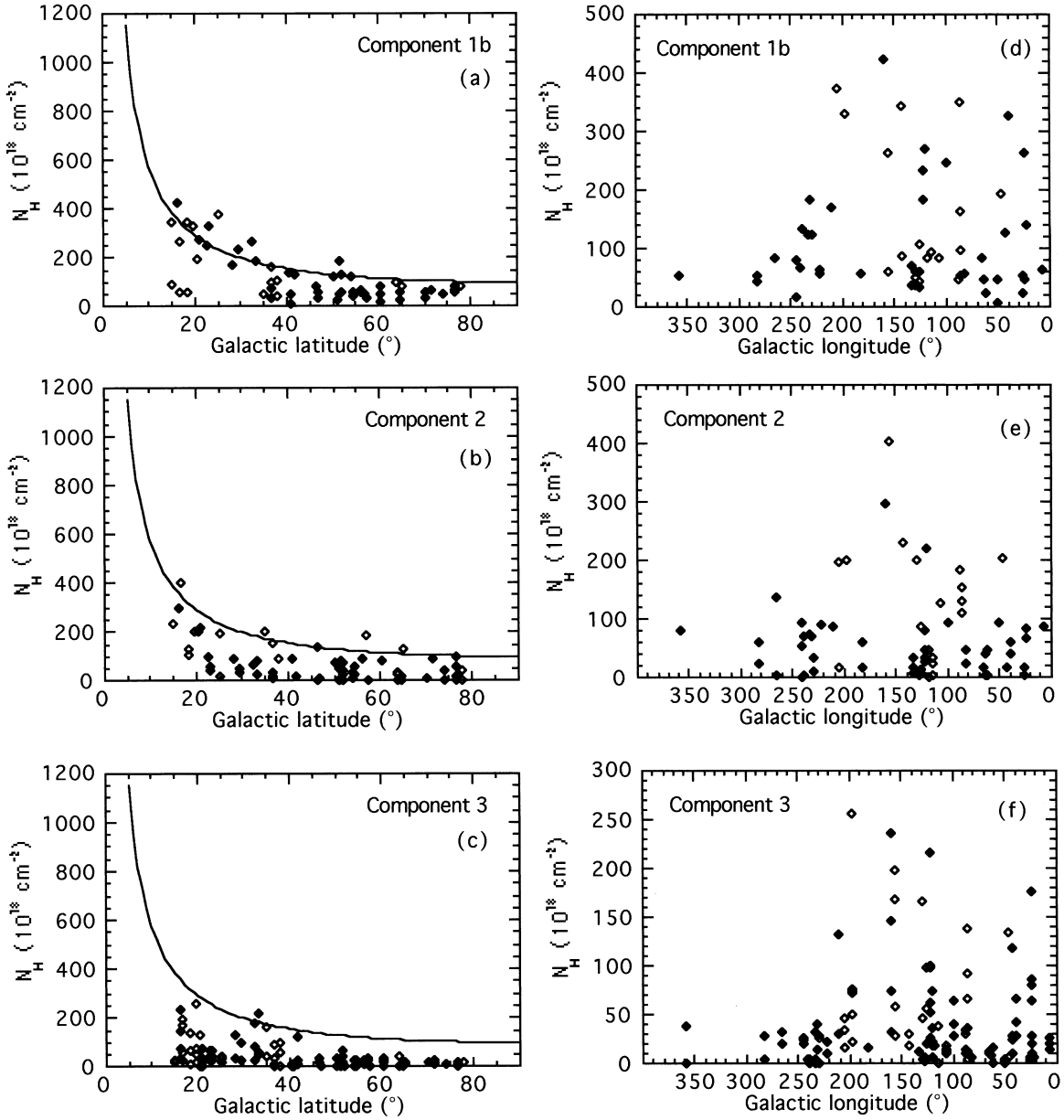

FIG. 6.—Latitude and longitude dependence of column densities for components 1b, 2, and 3 from the L-D data random direction sample. Curves representing a csc b dependence are indicated. Filled symbols represent positive latitudes, and open symbols, negative latitudes.

5.4. *Data toward a Thin Filament*

During a study of *IRAS* 100 μm maps, the presence of a very straight thin film was noted by one of us (G. L. V.). This filament terminates in two complex structures suggesting a twisted filament seen end-on, and it became the subject of an H I mapping program in order to determine whether the filament showed rolling motion consistent with the Bennett pinch phenomenon discussed by Verschuur (1995b). First, data from the L-D Survey over an area bounded by $l = 55°$–$61°$ and $b = 63°$–$72°$ were Gaussian-analyzed. This sample yielded a total of 247 profiles separated by 0°.5 in each coordinate. At these latitudes, profiles at half-integral longitudes in the L-D Survey were produced by interpolating between profiles separated by 1°, but nevertheless all the profiles in the sample were used. The Gaussian analysis was performed at least twice to determine whether any subjective trends appeared in the statistics of the line widths. None were noticed.

In all, some 1695 Gaussians were fitted to the data, but only 1145 of these that pertain to components with peak brightness temperatures above 0.1 K and center velocity greater than -50 km s^{-1} were included in the statistics. For the weaker components too much uncertainty entered into the fitting procedure, and the velocity cutoff was determined by the peculiar shape of the profiles, which indicate the presence of a second peak in the profiles around -55 km s^{-1}. Figure 4*e* shows the histogram of line widths for these data. The peaks in component widths clearly correspond to the three major line width categories described above. These are summarized in Table 7. Component 1b is 33.2 km s^{-1} wide, component 2 is 12.6 km s^{-1} wide, and component 3 is 4.6 km s^{-1} wide.

TABLE 7

H I Profile Line Widths in Component Categories

Sample	Component 1a	Component 1b	Component 2	Component 3
From L-D Survey Data				
Random directions.....	...	32.8 ± 1.8	12.8 ± 1.2	5.2 ± 1.3
L-D data for LJM86[a] directions.....	50.2 ± 1.0	29.9 ± 1.8	13.5 ± 1.7	5.3 ± 1.7
H0827+10.....	...	30.9 ± 3.7	11.3 ± 1.1	5.7 ± 1.6
H0928+02.....	...	30.7 ± 0.8	13.2 ± 0.6	4.7 ± 1.1
H1025+05.....	...	31.2 ± 2.1	14.9 ± 1.5	5.8 ± 1.0
UMa	...	30.7 ± 1.2	9.0 ± 1.2	5.0 ± 1.1
Thin filament	...	33.2 ± 3.2	12.6 ± 2.6	4.6 ± 1.5
From LJM86 data	50.1 ± 0.8	32.0 ± 1.9	13.5 ± 1.3	5.2 ± 1.2
Average	50.1 ± 0.6	31.0 ± 0.5	12.6 ± 0.4	5.2 ± 0.4
Other Data Sets				
Verschuur 1995c profile data	...	33.8 ± 5.3	13.6 ± 2.1	5.0 ± 1.8
Verschuur & Schmelz 1989	...	36.3 ± 4.1	12.0 ± 2.8	4.0 ± 4.1
Thin filament	...	33.1 ± 2.8	13.6 ± 1.1	6.2 ± 1.6
Average for all	50.1 ± 0.6	31.0 ± 0.5	12.8 ± 0.4	5.2 ± 0.4

Note—Line widths in kilometers per second.
[a] Lockman et al. 1986.

A narrower stretch of sky along the filament itself was subsequently mapped on the 140 foot radio telescope of the NRAO in 1997 February, and 36 profiles obtained with 8′ separation for full angular sampling gave 179 Gaussian components. Their line width histogram is shown in Figure 4*f*, and the average line widths are given in Table 7. They are essentially the same as those found from the L-D Survey data.

5.5. *Two Further Data Sets*

For the purposes of this study, an analysis done on a set of H I profiles obtained with long integrations (~36 minutes each) was reexamined. The relevant data were obtained in 1992 during the 21 cm Zeeman experiment (Verschuur 1995c) using the 140 foot radio telescope of the NRAO. The Gaussian analysis was performed at the telescope and 310 Gaussians identified in 75 profiles, and at the time no preconceived notions existed as to what would be done with the results of that analysis. The average values for the component categories are shown in Table 7 and rather dramatically emphasize the existence of the primary line width components.

TABLE 8

Directions of Profiles from the Lockman et al. (1986) Sample

Longitude	Latitude	Comment
North Galactic pole		
200.0	86.0	
133.5	85.5	
85.5	76.0	
56.0	66.0	
100.5	65.5	
182.0	58.0	
152.0	53.0	Their Fig. 3; (−31′,−40′)
151.0	52.5	Their Fig. 3; (−25′,0′)
151.5	52.0	Their Fig. 3; (−65′,0′)
160.0	50.0	
133.5	−85.5	

Note—Positions rounded off for use with L-D Survey database.

The next entry in Table 7 summarizes the mean line width for the three major component categories from the data of Verschuur & Schmelz (1989), who presented a variety of line width histograms.

5.6. *The Line Width Components: A Summary*

Examination of Figure 4 shows that the three line width regimes described by Verschuur & Magnani (1994) exist in all the L-D Survey sidelobe-corrected profiles studied here, which were all observed at intermediate and high Galactic latitudes. In addition, a fourth component is recognized in profiles obtained in directions of low H I column density. Table 7 summarizes the mean line widths for each component from all the above data sets. The average line width for component 1a is 50.1 ± 0.6 km s^{-1}, for component 1b it is 31.2 ± 0.5 km s^{-1}, for component 2 it is 12.8 ± 0.4 km s^{-1}, for the component 3 it is 5.2 ± 0.4 km s^{-1}.

6. A NOTE ON H I COLUMN DENSITIES

In order to further illustrate the quality and significance of the Gaussian fitting, Table 9 shows the mean line width and the mean H I column densities associated with the various component categories for the data from the L-D Survey for samples of random and low-density directions. In addition, the results of two separate analyses for the L-D Survey random direction sample are shown. While the scatter on the column density values in each category is large, a trend is clearly evident in the data. For the profiles

TABLE 9

H I Column Densities in Component Categories: L-D Data

Category	Mean Line Width (km s^{-1})		Mean Column Density (10^{18} cm^{-2})	
	First Analysis	Second Analysis	First Analysis	Second Analysis
Random directions:				
Component 3 (3.0–9.9 km s^{-1})	5.2 ± 1.3	5.4 ± 1.7	50.1 ± 62.8	43.9 ± 54.4
Component 2 (11.0–15.9 km s^{-1}).....	12.8 ± 1.2	13.2 ± 1.1	77.3 ± 79.4	72.0 ± 79.1
Component 1b (28–39 km s^{-1})	32.8 ± 1.8	33.0 ± 2.5	141 ± 110	131 ± 110
LJM directions:				
Component 3 (3.0–9.9 km s^{-1})	5.3 ± 1.7	...	4.7 ± 5.7	...
Component 2 (11.0–15.9 km s^{-1}).....	13.5 ± 1.7	...	13.2 ± 8.9	...
Component 1b (28–39 km s^{-1})	29.9 ± 1.8	...	23.2 ± 19.1	...
Component 1a (48–51 km s^{-1})	50.2 ± 1.0	...	44.5 ± 19.8	...

Note—Line width ranges used for averaging are shown in parentheses.

in directions of low column density the broadest component 1a, contains 50% of the H I emission. In the random directions sampled, component 1b contains 52% of the H I emission. Since the even broader component 1a has not been identified in these data, it raises the question whether it may be present but too weak to be identified in our analysis. Were it to contain as much column density as component 1b its peak brightness temperature should be of order 1 K, which means it should have been detectable in the L-D data. This implies that perhaps component 1a is only visible in directions of low column density for physical reasons related to the relative absence of the other components, an issue that deserves closer consideration.

7. COMPARISON WITH THE RESULTS OF SPITZER & FITZPATRICK (1993)

Ultraviolet *Hubble Space Telescope* spectral line observations toward the Galactic halo star HD 93521 (at $l = 183°$, $b = +62°$) have been published by Spitzer & Fitzpatrick (1993), who compared their data with an H I profile from Danly et al. (1992). This emission profile is very complex for so high a Galactic latitude. Spitzer & Fitzpatrick (1993) fitted 10 components, with their choice of parameters directly influenced by their need to account for the ultraviolet spectral lines associated with S I, S II, Si II, Mg II, Mn II, C II, and Fe II, as well as optical lines from Na I, Ca II, and Ti II.

We have examined the L-D Survey H I profile for this direction with a view to performing a Gaussian fit in the manner used throughout our study. In Figure 5*a* the two profiles are compared. There is good agreement at velocities more negative than −15 km s^{-1}, but above that the two profiles are very different, too different, we think, to be accounted for only by beamwidth differences. This may be an artifact of the sidelobe correction used by Danly et al. (1992) relative to that derived by Hartmann (1994). The results of Gaussian fitting to the L-D Survey profile is shown in Figure 5*b* and summarized in Table 10, where the data are compared with the parameters given by Spitzer & Fitzpatrick (1993). The general pattern of Gaussians fitted to this L-D Survey profile mimics that found in other directions where two very distinct peaks in H I emission are found, one at near-zero velocity and the other in the IVC regime of −50 km s^{-1}. Component 1b and component 2 can be fitted to both parts of the profile, and narrow lines often overlie both.

If we recognize that the profiles shown in Figure 5*a* differ significantly at velocities greater than −15 km s^{-1}, the Gaussian fits to the new data (Fig. 5*b*) summarized in Table agree fairly well in center velocity but not as well for the line widths. The reason rests in a different approach to the Gaussian fitting by Spitzer & Fitzpatrick (1993) compared with our study. We have argued that the underlying broad components are pervasive and need to be fitted before attempting to account for details in spectral shape. Spitzer

TABLE 10

Comparison of Gaussian Fits for the l = 183°, b = 62° Profile

Spitzer and Fitzpatrick (1993)				Analysis of L-D Survey Profile				
Comp. Number	Velocity l.s.r. (km s^{-1})	Line-width (km s^{-1})	Log N_H) (cm^{-2})	Peak (°K)	Velocity l.s.r. (km s^{-1})	Line-width (km s^{-1})	Log N_H) (cm^{-2})	Comment
1	−66.3	15.5	18.5	0.22	−64.9	11.5	18.7	Comp 2
2	−56.7	12.8	19.4	0.98	−54.2	14.9	19.4	Comp 2
3	−50.1	15.6	19.2	0.14	−50.8	30.8	18.9	Comp 1b
4	−37.7	17.8	18.9	0.24	−39.5	10.2	18.6	
5	−28.0	8.8	18.4	10.8				very weak
6	−17.1	10.8	19.3	0.85	−14.4	14.0	19.3	Comp 2
7	−9.1	11.8	19.4	12.1				see Fig. 16
8	3.6	12.1	19.3	0.61	−3.8	34.0	19.6	Comp 1b
9	8.4	15.1	18.8					see Fig. 16
7A	−7.9	3.6	18.8	0.26	−7.8	5.0	18.4	Comp 3

& Fitzpatrick (1993), on the other hand, were driven to fit narrow components, which they expected to exist based on UV and optical data. We attempted a Gaussian fit to their profile but were unable to do so because so much depended on fitting to small changes of slope in the profile that could not be distinguished from noise and, in the context of the comparison with the L-D Survey profile above, from possible errors in the sidelobe correction to the Danly et al. (1992) profile referred to before.

The column densities for those components that were fitted to the L-D Survey profile for this direction are similar to the Spitzer & Fitzpatrick (1993) fits, where we agree on the center velocities of individual Gaussians. These are numbered components 1–4 and 6 in Table 10. We find no need for a component 5 and no agreement with their numbered components 7–9, because the two profiles differ so much over the relevant velocity range (Fig. 5*a*), while component 7A appears in both data sets.

This comparison has been offered to raise a key issue. The Spitzer & Fitzpatrick (1993) Gaussian fit to the H I profile did not allow for the possible existence of pervasive broad underlying components, which define the low-level emission in typical H I profiles described here. They approached their Gaussian fitting by beginning with narrow features about which they had a priori information from UV lines. Also, we have found that Gaussian fitting to complex profiles to obtain physically meaningful results, such as making sure that the broad components vary smoothly over an area of sky around a given direction, requires taking account of the H I structure over that area. This is why we have avoided such profiles in our study. In complex areas with bright emission, Gaussian fitting cannot be successfully accomplished by looking at a single profile. In general, if meaningful data are the goal, Gaussian analysis of complex H I profiles should be avoided! If this cannot be avoided, the structure of a given profile in the context of its surroundings should, at the very least, be considered.

The general agreement found for the column densities for the components 1–4, 6, and 7A of Spitzer & Fitzpatrick (1993) validates that aspect of their discussion that concerned this parameter. Our study, however, stresses the nature of the line widths. Also, our study did not include a Gaussian analysis of any profiles that required 10 or 11 Gaussian to specify the line shape. The identification of the component categories referred to in our report is based on profiles that are inherently simpler to analyze into Gaussians than the profile studied by Spitzer & Fitzpatrick (1993).

8. DISCUSSION: ORIGIN OF THE COMPONENTS

In order to investigate in what regions of space the various components might arise, the H I column density dependence on latitude and longitude were examined for the L-D Survey random direction sample. The results are shown in Figure 6. In the latitude plots a cosecant latitude curve is shown for comparison, and it is evident that components 1b and 2 are consistent with their arising in the disk of the Galaxy. The latitude dependence of column density for the component 3 sample suggests a two-tiered structure with increased values and larger scatter below latitude 40° and low values with less scatter above that.

The dependence of column density on longitude shows no clear pattern at all, such as might be expected for a halo population, which would cause systematically higher column densities around longitude zero and lower values toward the anticenter, where overall path lengths would be much shorter. No such trend is evident in any of the data. Thus, we conclude that all three components have their origin in the disk of the Galaxy.

9. CONCLUSIONS

We have presented evidence that neutral hydrogen emission profiles produced by gas in the local interstellar medium are characterized by three, and probably four, line width regimes. Dominant and pervasive features have widths of order 5.2, 13, and 31 km s^{-1}, and limited evidence has been found for a very broad component ~ 50 km s^{-1} wide. The data are consistent with all three major component line width regimes caused by gas confined to the Galactic disk. A simplistic interpretation might suggest that the gas is somehow found in "clouds" in pressure equilibrium with a hierarchy of structures, but we are unable to formulate a reasonable picture along these lines. Instead, we note that the line width regimes show a striking resemblance to a set of velocity regimes described by a plasma physical mechanism called the critical ionization phenomenon.

When a low-density neutral gas flows through a low-density plasma permeated by a magnetic field, neutral atoms ionize when their velocity relative to the plasma is such that their kinetic energy exceeds the ionization potential of the neutrals. The magnitudes of the critical ionization velocities (CIVs) for common atomic species fall into three distinct bands. Band I includes hydrogen, with a CIV of 51 km s^{-1}, and He, with a CIV of 34 km s^{-1}, band II includes C, N, and O, with CIVs around 13.5 km s^{-1}; and band III includes heavier atomic species such as Na and Ca, with CIVs around 6 km s^{-1}. We regard the coincidence between the magnitudes of the CIVs for common interstellar atoms and H I line width regimes discussed above as more than fortuitous and in a subsequent paper will conclude that H I profile shapes are affected by the CIV phenomenon in interstellar space. This implies the existence of a previously unrecognized source of ionization that needs to be taken into account in the study of interstellar gasdynamics, physics, and chemistry.

We owe a great debt of gratitude to W. B. Burton, Steve West, and Dap Hartmann for making available H I emission profiles from the magnificent Leiden-Dwingeloo all-sky H I survey; and to Joan T. Schmelz for a critical reading of an early version of the manuscript.

REFERENCES

Alfvén, H. 1942, Stockholms Obs. Ann., 14, No. 2
———. 1954. On the Origin of the Solar System (Oxford: Clarendon)
———. 1960, New Sci., 7, 1188
Boulanger, F., & Perault, M. 1988, ApJ, 330, 350
Brenning, N. 1992a, IEEE Trans. Plasma. Sci., 20, 778
———. 1992b, Space Sci. Rev., 59, 209
Brown, A. G. A., Hartmann, D., & Burton, W. B. 1995, A&A, 300, 903
Burton, W. B. 1985, A&AS, 62, 365
Burton, W. B., & te Lintel Hekkert, P. 1985, A&AS, 62, 645
Colomb, F. R., Pöpell, W. G. L., & Heiles, C. 1980, A&AS, 40, 47
Danly, L., Lockman, F. J., Meade, M. R., & Savage, B. D. 1992, ApJS, 81, 125

Hartmann, D. 1994, Ph.D. thesis, Univ. Leiden
Hartmann, D., & Burton, W. B. 1997, Atlas of Galactic Neutral Hydrogen, (Cambridge: Cambridge Univ. Press L-D Survey)
Heiles, C., & Habing, H. J. 1974, A&AS, 14, 1
Kalberla, P. M. W., Westphalen, G., Mebold, U., Hartmann, D., & Burton, W. B. 1998, A&A, 332, L61
Lockman, J., Jahoda, K., & McCammon, D. 1986, ApJ, 302, 432
Peratt, A. L., & Verschuur, G. L. 1998, in 1998 IEEE International Conference on Plasma Science (Piscataway, NJ: IEEE), 129
———. 1999, in preparation
Spitzer, L., & Fitzpatrick, E. L. 1993, ApJ, 409, 299
Stark, A. A., Gammie, C. F., Wilson, R. W., Bally, J., Linke, R. A., Heiles, C., & Hurwitz, M. 1992, ApJS, 79, 77
Verschuur, G. L. 1974a, ApJS, 27, 65
———. 1974b, ApJS, 27, 283
Verschuur, G. L. 1991a, Ap&SS, 185, 137
———. 1991b, Ap&SS, 185, 305
———. 1994, in ASP Conf. Ser. 58, The First Symposium on the Infrared Cirrus and Diffuse Interstellar Clouds, ed. R. M. Cutri & W. Latter (San Francisco: ASP), 184
———. Plasma Astrophysics and Cosmology (Dordrecht: Kluwer), 187
———. 1995b, Ap&SS, 227, 187
———. 1995c, ApJ, 451, 624
Verschuur, G. L., & Magnani, L. 1994, AJ, 107, 287
Verschuur, G. L., Rickard, L. J., Verter, F., Pound, M. W., & Leisawitz, D. 1992, ApJ, 390, 514
Verschuur, G. L., & Schmelz, J. T. 1989, AJ, 98, 267
Weaver, H. F., & Williams, D. R. W. 1973, A&AS, 8, 1
Westerhout, G. 1966, Maryland–Green Bank Galactic 21-cm Line Survey (College Park: Univ. Maryland)